TABLE OF CONTENTS

LIST OF FIGURES

LIST OF TABLES

Chapter 1 Per-Pixel Calibration and 3D Reconstruction on GPU

1.1 *RGBD* to $X^C Y^C Z^C RGB$

As described in chapter **??**, there are applications like SLAM and KinectFusion that require D to be converted into $X^C Y^C Z^C$ coordinates on a per-pixel basis. From Chapter **??**, we know that the depth sensor measures Z^C, and a pinhole camera model (more specifically the intrinsic matrix) in homogeneous coordinates offers the relationship between Z^C and X^C/Y^C respectively. In this section, we will introduce how to generate the camera space 3D coordinates without calibration, and draw a camera space 3D reconstruction on GPU using a KinectV2 camera.

The KinectV2 depth sensor measures Z^C in millimeter and supports its positive data in unsigned-short data-type. Those data will be automatically converted into single-floating type with its range from 0.0f to +1.0f when uploaded onto GPU. Considering that in practical Ds from KinectV2 are always positive whereas Z^Cs should be always negative, we will add a negative sign in the un-scaling step to recover the Z^C in metric on GPU:

$$Z^C[m,n] = -\beta D[m,n], \tag{1.1}$$

where β constantly equals to 65535.0 (range of unsigned short in single-floating) for all pixels. Besides the depth stream, KinectV2 supports both of the horizontal and vertical field of view (FoV) that can help generate per-pixel X^C and Y^C, which share the same credits with the intrinsic parameters in a pinhole camera model. Figure 1.1 shows an intuitive

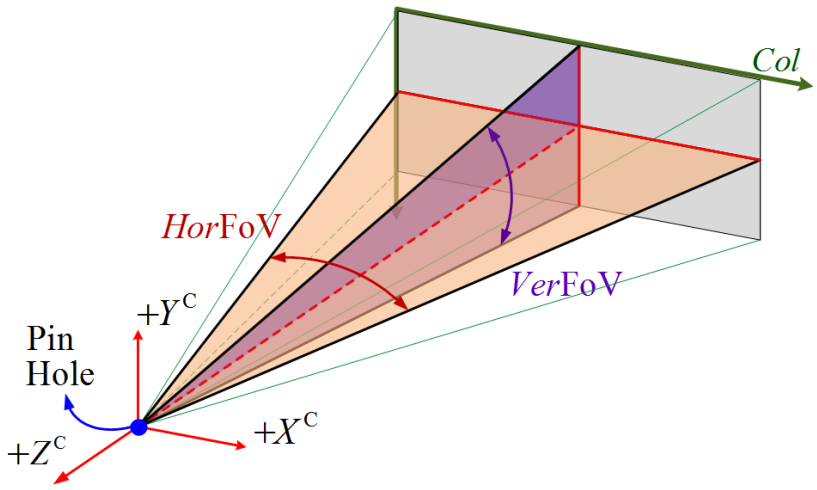

Figure 1.1: Field of View in Pinhole-Camera Model

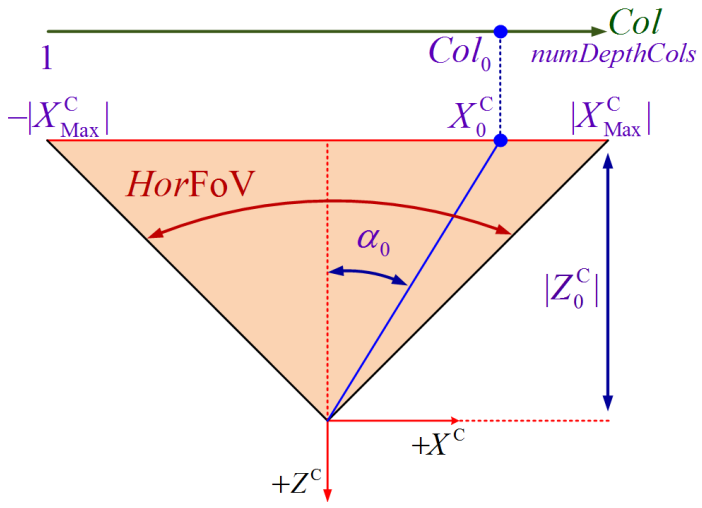

Figure 1.2: map Col to X^C via horizontal FoV

view of the horizontal and vertical FoVs in a pinhole camera model, based on which we can derive the X^C and Y^C values given a random Z^C value on the per-pixels basis. Assuming the depth sensor, with its size numDepthRows by numDepthCols, is observing right perpendicularly to a wall where all pixels share the same $|Z^C_0|$ from the sensor to the wall. Talking about the horizontal FoV only, it is easy to get the range of the camera space FoV along X^C-axis from $-|X^C_{\text{Max}}|$ to $|X^C_{\text{Max}}|$, as shown in fig. 1.2. The horizontal range value $|X^C_{\text{Max}}|$ depends on $|Z^C_0|$ and the horizontal FoV, given by:

$$|X^C_{\text{Max}}| = |Z^C_0| \cdot tan(horFov/2) \tag{1.2}$$

where the pixel observing on $X^C = |X^C_{\text{Max}}|$ has its column address of numDepthCols. Similarly, given a random pixel of column address Col_0, its horizontal view X^C_0 could be expressed based on its own horizontal view angle α_0.

$$|X^C_0| = |Z^C_0| \cdot tan(\alpha_0) \tag{1.3}$$

To combine eqn. 1.2 and eqn. (1.4), we get

$$\frac{X^C_0}{|X^C_{\text{Max}}|} = \frac{tan(\alpha_0)}{tan(horFov/2)} = \frac{Col_0}{numDepthCols} - 0.5\,, \tag{1.4}$$

which shows how to get the per-pixel X^C_0 from $|X^C_{\text{Max}}|$ based on its column address, while $|X^C_{\text{Max}}|$ depends on the depth sensor's horizontal filed of view. It is intuitively better to change eqn. (1.4) a little by substituting $|X^C_{\text{Max}}|$ with eqn. (1.2) such that we can get eqn. (1.5),

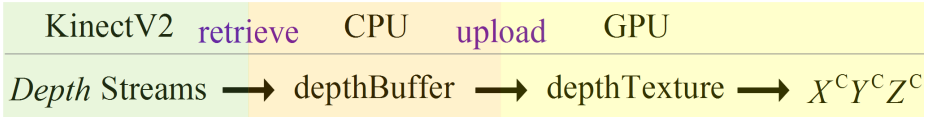

Figure 1.3: Diagram for Camera Space 3D Reconstruction without calibration

a proportional per-pixel mapping based on the column addresses from Z^C to X^C.

$$X^C[m,n] = tan(horFov/2) \cdot (\frac{n}{numDepthCols} - 0.5) \cdot |Z^C[m,n]|\,, \tag{1.5}$$

where $[m,n]$ is the discrete space *row* and *column* coordinate of each pixel in the depth sensor. Similarly, we can also get the proportional per-pixel mapping from Z^C to Y^C, based on the vertical FoV and row addresses.

$$Y^C[m,n] = tan(verFov/2) \cdot (\frac{m}{numDepthRows} - 0.5) \cdot |Z^C[m,n]| \tag{1.6}$$

Note that, *horFov* and *verFov* are constant during image processing, such that the mapping functions from per-pixel Z^C to per-pixel X^C/Y^C totally depend on a pixel's address $[m,n]$. Therefore eqn. (1.5) and eqn. (1.6) could be expressed as

$$\begin{aligned} X^C[m,n] &= a[m,n] \cdot |Z^C[m,n]| \\ Y^C[m,n] &= b[m,n] \cdot |Z^C[m,n]| \end{aligned} \tag{1.7}$$

where

$$\begin{aligned} a[m,n] &= tan(horFov/2) \cdot (\frac{n}{numDepthCols} - 0.5) \\ b[m,n] &= tan(verFov/2) \cdot (\frac{m}{numDepthRows} - 0.5)\,. \end{aligned} \tag{1.8}$$

Now that we have the per-pixel mapping from Z^C to $X^C Y^C$, it is time to draw the camera space 3D image on GPU. Figure 1.3 shows the streams flow diagram. We will retrieve *Depth* streams from the KinectV2 camera, save them into corresponding buffers on CPU and upload the the streams onto GPU as textures. Then the per-pixel's camera space 3D coordinates $X^C Y^C Z^C$ will be generated during its fragment-shader processing from depth texture based on eqn. (1.7). The fragment shader is programmed as below.

```
uniform sampler2D qt_depthTexture;
uniform sampler2D qt_spherTexture;

layout(location  =0,index  =0)out  vec4 qt_fragColor;
void main()
```

```
{
    ivec2 textureCoordinate=ivec2( gl_FragCoord.x, gl_FragCoord.y);

    floatz = texelFetch(qt_depthTexture,textureCoordinate,0).r *65535.0;
    vec4 a = texelFetch(qt_spherTexture,textureCoordinate,0);

    qt_fragColor.x = -z*a.r;
    qt_fragColor.y = -z*a.g;
    qt_fragColor.z = -z;
}
```

The uniform *qt_spherTexture* is a Z^C to X^C/Y^C proportional mapping texture, which contains the per-pixel parameters a/b based on eqn. (1.8). Note that we add three negative signs in front of $X^C Y^C Z^C$ respectively to account for the pinhole-imaging. The whole parallel image processing above shows a natural 3D reconstruction on GPU. Figure 1.4 shows the view of camera space 3D reconstruction when observing uniform grid dots pattern on the flat wall. We can tell from the image that, this reconstruction is totally based on raw data, without calibration at all. Not only the radial dominated lens distortions are apparent in the front view, but the *depth distortion* is also material that cannot be ignored. Therefore, calibration must be done for an undistorted 3D image.

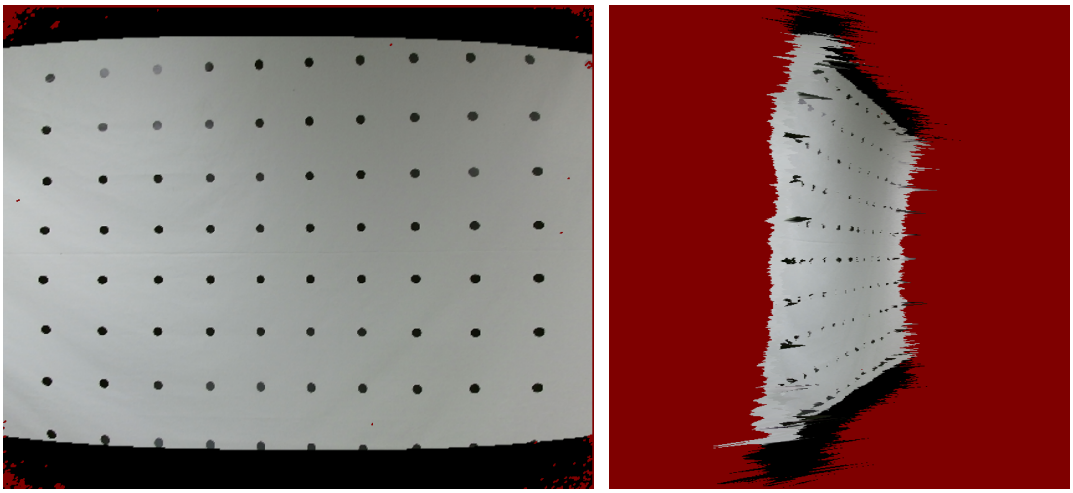

(a) Front View (b) Left View

Figure 1.4: Colored Camera Space 3D Reconstruction

1.2 Rail Calibration System

Talking about camera calibration, the pinhole camera matrix M will come up in most people's mind. As discussed in Chapter **??**, the pinhole-camera matrix M consists of an intrinsic matrix K and an extrinsic matrix $[R_{3*3}, T_{3*1}]$. The camera space 3D reconstruction method we discussed in section 1.1 utilizes horizontal and vertical field of view (FoV)s, which works in the same way with the intrinsic matrix K's principle. However, a camera's calibration needs external help from world space objects, which means neither of the FoVs nor intrinsic matrix K alone is able to do calibration, and extrinsic parameters that can link to world space are necessary in calibration.

Kai [1] did a good job on structured light 3D scanner parallel calibration on GPU, and derived the per-pixel beam equation (1.9) directly from a pinhole camera matrix M, which offers the possibility of natural 3D reconstruction on GPU similar to eqn. (1.7).

$$\begin{aligned} X^W[m,n] &= a[m,n]Z^W[m,n] + b[m,n] \\ Y^W[m,n] &= c[m,n]Z^W[m,n] + d[m,n] \end{aligned} \tag{1.9}$$

where $[m,n]$ is the discrete space *row* and *column* coordinate of each pixel in a M by N sensor. This per-pixel beam equation shows per-pixel linear mappings from Z^W to X^W/Y^W, and the per-pixel Z^W can be mapped from features of structured light. It is not specially proportional like eqn. (1.7), because it contains space translation infos from camera space to world space. Although it is in world space now and the intrinsic parameters are able to be determined, however, lens distortions are still not able to be handled. To make it ideal, we need to not only remove the lens distortions and *depth distortion*, but also realize the 3D reconstruction on GPU in a natural method similar to eqn. (1.9).

In this section, we will find a best-fit calibration system for a KinectV2 camera's natural calibration and reconstruction, which is able the handle both of lens distortion and *depth distortion*. To easily show 3D reconstruction in a parallel way on the GPU, we would like our calibration system to be able to offer a per-pixel mapping from D to Z^W, which then could be used to map to X^W/Y^W using eqn. (1.9). In this way, the *depth distortion* could also be corrected during the per-pixel D to Z^W mapping. Of all different kinds of calibration systems, a camera on rail system with a planar pattern on wall is finally decided, which offers a moving plane with respect to the camera when the camera moves along the rail. As fig. 1.5 shows, a canvas on which printed an uniform grid dots pattern is hung on the wall, and the rail is required to be perpendicular to the wall. The RGB-D camera waiting to calibrate is mounted on the slider. Note that, in this calibration system, the only unit that needs to be perpendicular to the wall is the rail, whereas the RGB-D camera has no

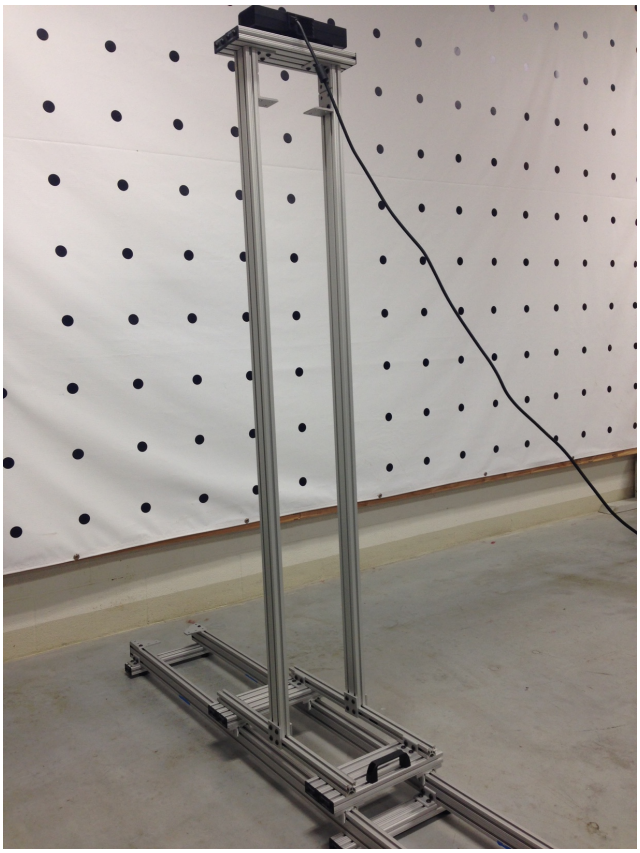

Figure 1.5: KinectV2 Calibration System

need to require its observation orientation. Because the per-pixel calibration requires only accurate world space coordinates which will be decided by the rail and the wall, whereas the camera's space is not considered at all. We will assign the pattern plane as the $X^W Y^W$ plane in world space, and the rail to be along with (not exactly on) Z^W-axis. The world coordinate is static with the camera on the slider.

Figure 1.6 shows one frame of NearIR $X^W Y^W Z^W$ 3D reconstruction, which can help a lot explaining how the world space origin is assigned. Inside the figure, both of the origin and Z-axis are high-lighted in blue, and the origin of world space is on the left end of the blue line. On the pattern plane with dot-clusters marked in circles, we can see one dot-cluster is high-lighted inside a thick circle, and its center point is where $X^W/Y^W = 0$. The dot-cluster which will be sitting on the Z^W-axis is the one whose center point is closest to the center pixel of the sensor. All pixels in this frame share the exact same Z^W, which is also why we require the rail to be perpendicular to the pattern. And the value of Z^W is measured by a laser distance measurer that static with the camera. The final origin of the world space will be decided by both of the camera's observing orientation and the laser distance measurer's position. This kind of world coordinate assignment is totally for

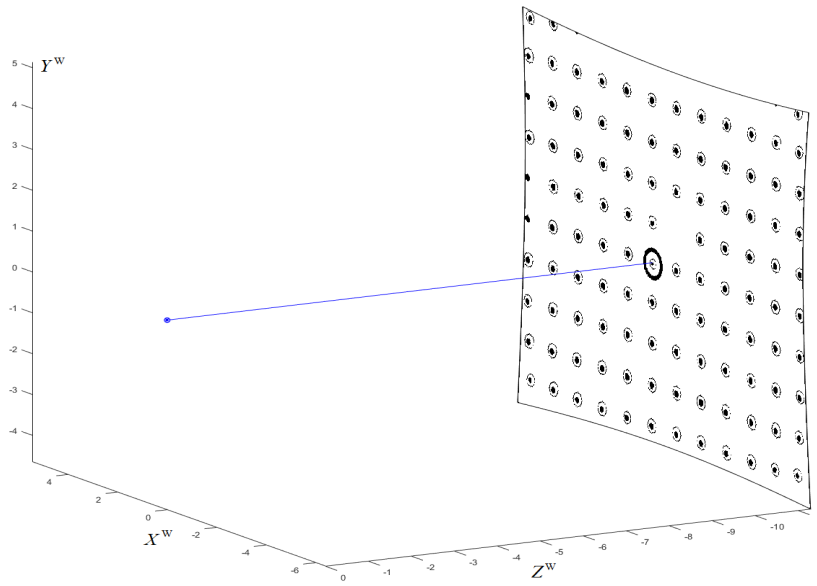

Figure 1.6: NearIR $X^W Y^W Z^W$ 3D Reconstruction

simplifying image processing during calibration. Practically, we do not even care where exactly the origin is, as long as the rail is perpendicular to the pattern and the distance measurer is static with the camera.

With this rail calibration system, infinite number of frames with infinite number of calibration points could be utilized for training a calibration model. Besides, as the slider moves along the rail, the amount and distribution of the grid dots captured by the camera will change, which means a dynamic pattern for calibration instead of static. With more and more dots walking into the camera's field of view under a certain rhythm as the slider moves further from the pattern plane, the dots (which will be extracted as calibration points) are able to cover all pixels of a sensor. What's more, a moving-plane system (multiple frames calibration instead of one frame calibration) makes it possible to do dense D to Z^W mapping, which will handle *depth distortion*.

1.3 Data Collection

With the calibration system built up and world coordinate assigned, we are now ready to calibrate. Z^W values for all pixels of every frame will be supported from external laser distance measurer. To simplify potential calculation during image processing, we assign the world coordinate *Unit One* based on the uniform grid dots patter, to be same with the side of pattern's unit-square. Concretely, the distance between every two adjacent dots' centers in real-world is 228mm. Therefore, Z^W = -Z(mm) / 228(mm), where Z is the vertical distance to the pattern plane in reality measured by the laser distance measurer.

Note that, Z^W values are always negative, based on the assignment of Cartesian world coordinate. The outline of calibration procedures is listed below.

1. Mount both of the camera and laser distance measurer onto the slider.
2. Move the slider to the nearest position to the pattern plane.
3. Record one frame of RGB data with one frame of NearIR data at this position.
    a) measure $|Z^W|$ using the laser distance measurer.
    b) grab RGB, NearIR and Depth streams from KinectV2 camera.
    c) extract center points (R/C) of dot-clusters from RGB and NearIR streams respectively.
    d) assign X^W/Y^W values to the extracted points, RGB and NearIR respectively.
    e) train and determine the best-fit high order polynomial model that map from *RC* to X^W/Y^W, RGB and NearIR respectively.
    f) generate dense X^W/Y^W for all pixels using the model, for NearIR and RGB streams respectively.
    g) save 2 frames of RGB and NearIR all pixels' data respectively: $X^W Y^W Z^W RGBD$ for RGB stream, and $X^W Y^W Z^W ID$ for NearIR stream, where the channel I in NearIR frame denotes *Intensity*.
4. Move the slider to the next position, and repeat step 3.

Concretely, we will record RGB and NearIR frames every 25mm at a time. During every time, $|Z^W|$ will be measured by the laser measurer and manually input into the shader at the very beginning of streams recording. After RGB, NearIR and Depth streams have been retrieved from KinectV2, we will utilize digital image processing (DIP) techniques to extract the center points' image addresses (R/C) of dot-clusters, and then determine a high-order polynomial model to build a mapping from *RC* to X^W/Y^W for dense world coordinates generation.

DIP Techniques on (R, C) Extraction

A robust DIP process on the extraction the points' addresses (R, C)s determines the accuracy of calibration. In this project, the extraction steps consist of gray-scaling, histogram equalization, adaptive thresholding and a little trick on black pixels counting. OpenGL is selected as the GPU image processing language. The default data type of steams saved on

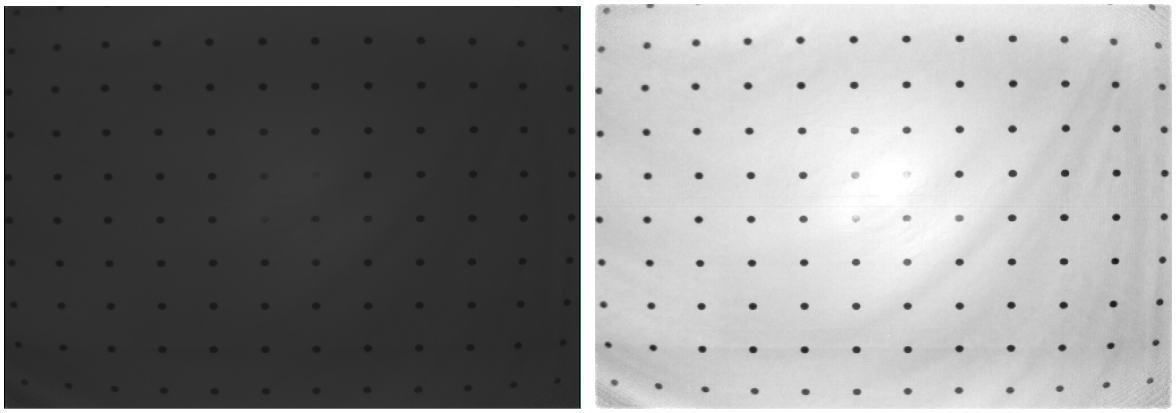

(a) Raw (b) Histogram Equalized

Figure 1.7: NearIR Streams before / after Histogram Equalization

GPU during processing is single-floating, with a range from 0 (balck) to 1 (white).

Gray-scaling is done to unify processing steps of both RGB and NearIR steams. For NearIR steam, its data contains only color gray and data will be saved on GPU as single-floating automatically. Whereas for RGB steam, a conversion from RGB to gray value is needed. Typically, there are three converting methods: lightness, average, and luminosity. The luminosity method is finally chosen as a human-friendly way for gray-scaling, give by

$$Intensity_{\_\text{gray}} = 0.21Red + 0.72Green + 0.07Blue\,, \tag{1.10}$$

which uses a weighted average value to account for human perception.

The pixel intensity values are automatically converted into single-floating type with its range from 0.0f to 1.0f, where "0.0f" means 100% black and "1.0f" means 100% white. In practical, NearIR steam image is always very dark, as shown in fig. 1.7a (with their intensity values every close to zero). In order to enhance the contrast of NearIR image for a better binarizing, histogram equalization technique is utilized to maximize the range of valid pixel intensity distributions. Same process is also compatible on the RGB stream. Commonly, Probability Mass Function (PMF) and Cumulative Distributive Function (CDF) will be calculated to determine the minimum valid intensity value ($floor$) and maximum valid value ($ceiling$) for rescaling, whereas tricks could be used by taking advantage of the GPU drawing properties.

PMF means the frequency of every valid intensity value for all of the pixels in an image. The calculation of PMF on GPU will be very similar to points' drawing process, both of which are on a per-pixel basis. Dividing all of the pixels in terms of their intensity values into N levels, every pixel belongs to one level of them, which is called gray level. With a

proper selection of N to make sure a good accuracy, the intensity value of a pixel could be expressed based on its gray level n

$$Intensity = n/N * (1.0f - 0.0f) + 0.0f = n/N, \tag{1.11}$$

where n and N are integers and $1 \leqslant n \leqslant N$. We will count PMF by drawing all pixels with "1" being their intensity (color) value, zero being y-axis all the time and their original intensity being their position on x-axis. Thus, PMF values at various gray levels could be drawn into a framebuffer object.

With PMF determined, CDF at gray leverl n could be calculated by

$$CDF(n) = \frac{sum}{N_{\text{\_Num of Total Pixels}}}, \tag{1.12}$$

where *sum* denotes the summation of PMF added up consecutively from gray leverl 1 till n, and N denotes how may pixels totally in a image. Then, the intensities $floor$ and $ceiling$ could be determined by

$$\begin{aligned} floor &= n_{\text{\_floor}}/N \\ ceiling &= n_{\text{\_ceiling}}/N \end{aligned} \tag{1.13}$$

through choosing appropriate CDFs, e.g., $CDF(n_{\text{\_floor}}) = 0.01$ and $CDF(n_{\text{\_ceiling}}) = 0.99$. Finally, a new intensity value of every single pixel in an image could be rescaled by

$$Intensity_{\text{\_new}} = \frac{Intensity_{\text{\_original}} - floor}{ceiling - floor}, \tag{1.14}$$

and the image will get a better contrast, as compared in fig. 1.7.

Affected by radial dominated lens distortions, the intensity value tend to decrease as the position of a pixel moves from the center of an image to the borders, in the case of observing a singular color view. Therefore, an adaptive thresholding process is needed, whereas using fixed thresholding will generate too much noise around borders. To segment the black dots from white background, we could simply subtract an image's background from an textured image, where the background comes from a blurring process of that image.There are three common types of blurring filters: mean filter, weighted average filter, and gaussian filter. Mean filter is selected for this background-aimed blurring process, because it has the smallest calculation and also a better effect of averaging than the others. After the blurred image containing background information is obtained, the binarizing (subtraction) process

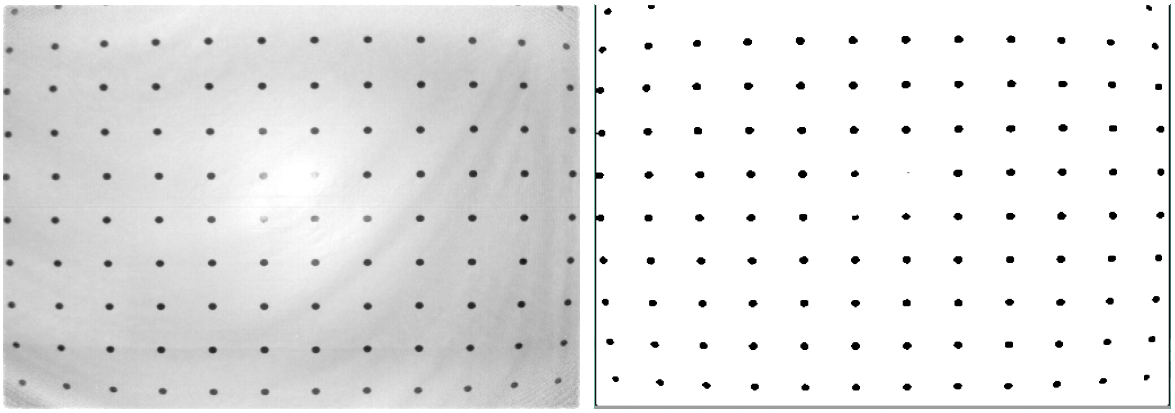

(a) Histogram Equalized (b) Binarized

Figure 1.8: NearIR Streams before / after Adaptive Thresholding

for every single pixel could be written as

$$Intensity_{\_\text{binarized}} = \begin{cases} 1, & I_{\_\text{textured}} - I_{\_\text{background}} - C_{\_\text{offset}} > 0 \\ 0, & else \end{cases}, \tag{1.15}$$

where I is short for $Intensity$ of every single pixel, and $C_{\_\text{offset}}$ is a small constant that could be adjusted depending on various thresholding situations. In this project, $C_{\_\text{offset}}$ is around 0.1.To sharpen the edge of the binarized image for a better "circle" shape detection, a median filter could be added as the last step of adaptive thresholding. As shown in Fig. 1.13, background is removed in the binarized image after adaptive thresholding.

After the adaptive thresholding, image data saved on GPU is now composed of circle-shaped "0"s within a background of "1"s. In order to locate the center of those "0"s circle, which is the center of captured round dot, it is necessary to know the edge of those circles. A trick is used to turn all of the edge data into markers that could lead a pathfinder to retrieve circle information.The idea that helps to mark edge data is to reassign pixels' values (intensity values) based on their surroundings. Using letter O to represent one single pixel in the center of a 3x3 pixels environment, and letters from A~H to represent surroundings, a mask of 9 cells for pixel value reassignment could be expressed as below.

E	A	F
B	O	C
G	D	H

To turn the surroundings *A*~*H* into marks, different weights will be assigned to them. Those markers with different weights have to be non-zero data, and should be counted as the edge-part of circles. Therefore, the first step is to inverse the binary image, generating an image that consists of circle-shaped "1"s distributed in a background of "0"s.After reversing, the next step is to assign weight to the surroundings. OpenGL offers convenient automatic data type conversion, which means the intensity values from "0" to "1" of single-floating data type save on GPU could be retrieved to CPU as unsigned-byte data type from "0" to "255". Considering a bitwise employment of markers, a binary calculation related weight assignment is used in the shader process for pixels. The intensity reassignment for every single pixel is expressed as the equation below.

$$I_{\text{\_Path Marked}} = I_{\text{\_Original}} * \frac{(128I_{\text{A}} + 64I_{\text{B}} + 32I_{\text{C}} + 16I_{\text{D}} + 8I_{\text{E}} + 4I_{\text{F}} + 2I_{\text{G}} + I_{\text{H}})}{255} \tag{1.16}$$

After this reassignment, the image is not binary any more. Every non-zero intensity value contains marked information of its surroundings, data at the edge of circles are now turned into fractions. In other words, the image data saved on GPU at the moment is composed of "0"s as background and "non-zero"s circles, which contains fractions at the edge and "1"s in the center.Now, it is time to discover dots through an inspection over the whole path-marked image, row by row and pixel by pixel. Considering that, a process of one single pixel in this step may affect the processes of the other pixels (which cannot be a parallel processing), it is necessary to do it on CPU. The single-floating image data will be retrieved from GPU to a buffer on CPU as unsigned-byte data, waiting for inspection. And correspondingly the new CPU image will have its "non-zero"s circles composed of fractions at the edge and "1"s in the center. Whenever a non-zero value is traced, a dot-circle is discovered and a singular-dot analysis could start. The first non-zero pixel will be called as an anchor, which means the beginning of a singular-dot analysis. During the singular-dot analysis beginning from the anchor, very connected valid (non-zero) pixel will be a stop, and a "stops-address" queue buffer is used to save addresses of both visited pixels and the following pixels waiting to be visited. On very visit of a pixel, there is a checking procedure to find out valid (non-zero) or not. Once valid, the following two steps are waiting to go. The first step is to sniff, looking for possible non-zero pixels around as the following stops. And the second step is to colonize this pixel, concretely, changing the non-zero intensity value to zero. Every non-zero pixel might be checked 1~4 times, but will be used to sniff for only once.

As for the sniffing step, base on the distribution table of *A*~*H* that has been discussed above and their corresponding weight given by equation 1.16, the markers *A*/*B*/*C*/*D* are

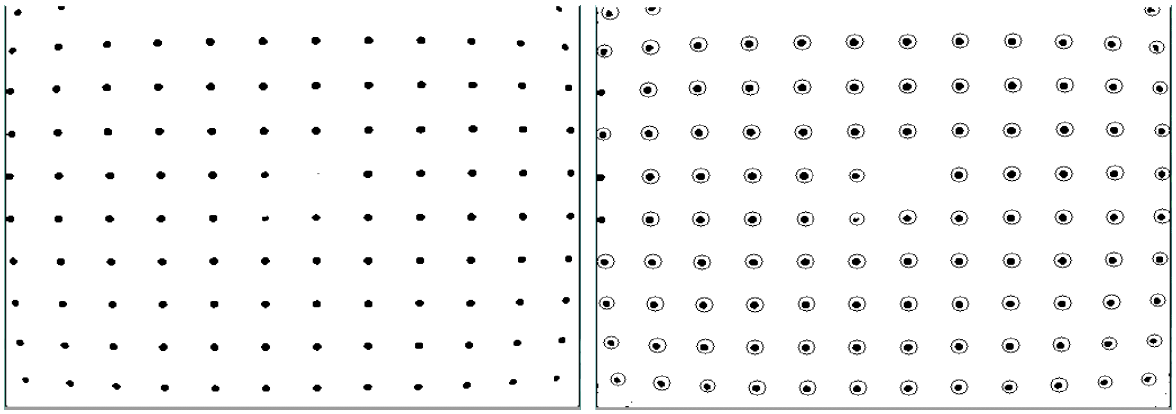

(a) before Extraction (b) Extracted and Marked

Figure 1.9: Valid Dot-Clusters Extracted in NearIR

valid (non-zero) as long as the intensity value of pixel O satisfies the following conditions shown as below.

$$
\begin{aligned}
&if\ (I_{\mathrm{O}}\ \&\ 0\mathrm{x}80 == 1), \quad then, \quad \text{marker } A \text{ is valid} \ \text{(go Up)} \\
&if\ (I_{\mathrm{O}}\ \&\ 0\mathrm{x}40 == 1), \quad then, \quad \text{marker } B \text{ is valid} \ \text{(go Left)} \\
&if\ (I_{\mathrm{O}}\ \&\ 0\mathrm{x}20 == 1), \quad then, \quad \text{marker } C \text{ is valid} \ \text{(go Right)} \\
&if\ (I_{\mathrm{O}}\ \&\ 0\mathrm{x}10 == 1), \quad then, \quad \text{marker } D \text{ is valid} \ \text{(go Down)}
\end{aligned}
$$

Once a valid marker is found, its address $(column, row)$ will be saved into the "stops-address" queue. One pixel's address might be saved for up to 4 times, but "colonizing" procedure will only happen once at the first time, so that the sniffing will stop once all of the connected valid pixels in a singular dot-cluster are colonized as zeros. In the second step "colonizing", I_{O} is changed to zero, variable *area* of this dot-cluster pluses one, and bounding data $RowMax$ / $RoxMin$ / $ColumnMax$ / $ColumnMin$ are also updated.Finally, the Round Dot Centers $(column, row)$ could be determined as the center of bounding boxes with their borders $RowMax$ / $RoxMin$ / $ColumnMax$ / $ColumnMin$. After potential noises being removed based on their corresponding *area* and *shape* (ratio of width and height), the data left are taken as valid dot-clusters. As shown in Fig. 1.9b, the centers of valid dot-clusters are marked within their corresponding homocentric circles.

(X^W, Y^W) Fitting based on Uniform Grid

With a list of image space points (R,C)s extracted, the following is to assign those points with their corresponding world coordinates (X^W, Y^W)s, so that we can get coordinate-pairs

to train a mapping model for dense $X^W Y^W$ generation. The world coordinates are based on the uniform grid. Taking the side of unit-square (distance between two adjacent dots) as "Unit One" in the world coordinates and one dot as the origin of plan $X^W Y^W$, all fitted X^W/Y^W values will be integers.

Ideally, a 3x3 perspective transformation matrix could help set a linear mapping between two different 2D coordinates, and 3 dot centers with known coordinates pair of (R,C) and (X^W, Y^W) are enough to determine the transformation matrix. Once four points with a squared-shape *R/C* distribution is found, a 3x3 perspective transformation matrix A could be determined by solving

$$\begin{bmatrix} zX^W \\ zY^W \\ z \end{bmatrix} = A \cdot \begin{bmatrix} C \\ R \\ 1 \end{bmatrix} = \begin{bmatrix} a_{11} & a_{12} & a_{13} \\ a_{21} & a_{22} & a_{23} \\ a_{31} & a_{32} & a_{33} \end{bmatrix} \cdot \begin{bmatrix} C \\ R \\ 1 \end{bmatrix} \tag{1.17}$$

where C and R are vectors consist of four squared-shape distributed points' addresses; X^W and Y^W are vectors consist of four points $(0,0)$, $(0,1)$, $(1,1)$, and $(1,0)$; z denotes the third axis in the homogenous system connecting two coordinates.

Deformed by lens distortions, the cluster centers in image plane are not uniformly distributed, and this 3x3 transformation matrix can only generate corresponding decimal X^W/Y^W values that are close integers. But in practical, the correct integer values X^W/Y^W could still be located through *Rounding*. Considering that a list of cluster centers' image coordinate (R,C)s will give many groups of four squared-shape distributed points, and each of them gives a different image coordinate distance will be mapped to the "Unit One" in world coordinates, we will traverse all of the possible groups of four squared-shape distributed points and pick out the group whose mapping matrix A generates the most points that are close to integers. In this way, we find the transformation matrix A can give the best "Unit One" distance in world coordinates. However, its generated point $X^W/Y^W = 0$ is usually not at the dot-cluster that is closest to the center of cameras' FoV. A translation matrix T could be used to refine the transformation matrix A and help to translate the origin point to be at the dot cluster we want, given by

$$A_{\text{\_refined}} = T \cdot A = \begin{bmatrix} 1 & 0 & -X_{\text{\_Zero\_A}} \\ 0 & 1 & -Y_{\text{\_Zero\_A}} \\ 0 & 0 & 1 \end{bmatrix} \cdot A \ , \tag{1.18}$$

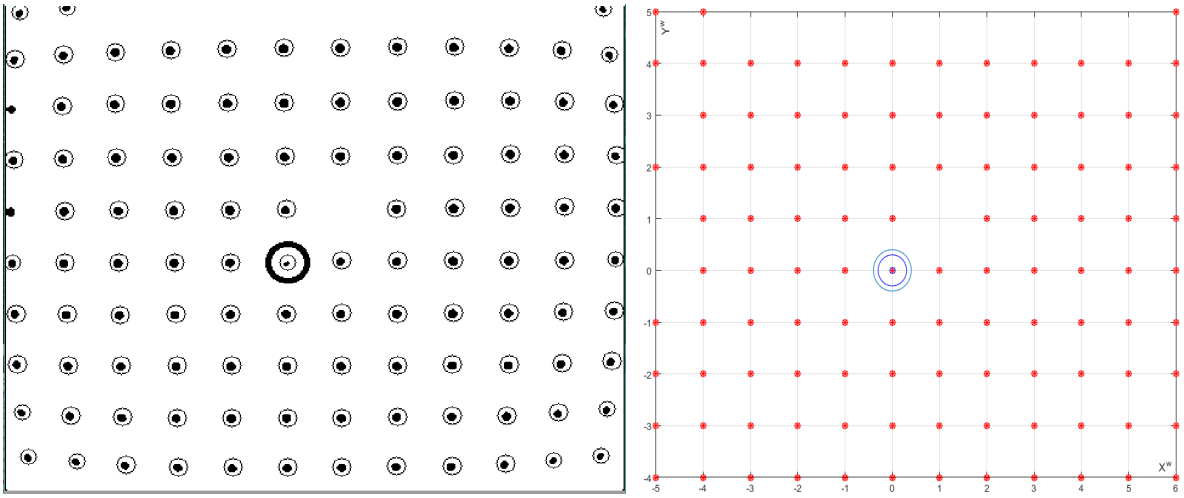

(a) ImagePlane Coordinate (b) World Coordinate

Figure 1.10: Coordinates-Pairs: (R,C)s and (X^W, Y^W)s

where the integer world coordinate point $(X_{\text{\_Zero\_A}}, Y_{\text{\_Zero\_A}})$ are rounded world space coordinates, written as

$$\begin{bmatrix} zX_{\text{\_Zero\_A}} \\ zY_{\text{\_Zero\_A}} \\ z \end{bmatrix} = A \cdot \begin{bmatrix} C_{\text{\_center}} \\ R_{\text{\_center}} \\ 1 \end{bmatrix} \tag{1.19}$$

which are mapped from the center point $(C_{\text{\_center}}, R_{\text{\_center}})$ of FoV in image plane by the transformation matrix A. Eventually, the refined transformation matrix eventually generates a list of world coordinate points (X^W, Y^W)s that correspond to image coordinates $(column, row)$s. As shown in fig. 1.10b, world coordinates are integers and the origin (blue circle) is chosen as where the center-closest dot-cluster is sitting.

Dense X^W/Y^W Generation

The generation of undistorted dense $X^W Y^W$ needs to consider lens distortion removal. In the traditional calibration method, world space $X^{\text{W}}/Y^{\text{W}}/Z^{\text{W}}$ are mapped to undistorted (R',C') by linear pinhole camera matrix M. And then the undistortion step from undistorted (R',C') to distorted (R,C) is done by eqn. **??**, which uses a high order (higher than 2nd order) polynomial equation. Assuming that there is a high order mapping relationship directly from the distorted image space (R,C) to world space $(X^{\text{W}}, Y^{\text{W}})$, we will do different orders of two-dimensional polynomial prototypes in Matlab using its application of "Curve Fitting Toolbox", and then decide a best-fit mapping model with a high accuracy and a relative small number of parameters.

A two-dimensional polynomial model means surface mapping between two different spaces. Equation. (1.17) (perspective correction) as 1^{st} order polynomial mapping is not able to handle lens distortions. The second order polynomial mapping has 2x6=12 parameters, written as

$$\begin{aligned} X^W &= a_{11}C^2 + a_{12}CR + a_{13}R^2 + a_{14}C + a_{15}R + a_{16} \\ Y^W &= a_{21}C^2 + a_{22}CR + a_{23}R^2 + a_{24}C + a_{25}R + a_{26}\,, \end{aligned} \tag{1.20}$$

and similarly, the fourth order polynomial mapping has 2x15=30 parameters, given by

$$\begin{aligned} X^W &= a_{11}C^4 + a_{12}C^3R + a_{13}C^2R^2 + a_{14}CR^3 + a_{15}R^4 + a_{16}C^3 + a_{17}C^2R \\ &\quad + a_{18}CR^2 + a_{19}R^3 + a_{110}C^2 + a_{111}CR + a_{112}R^2 + a_{113}C + a_{114}R + a_{115} \\ Y^W &= a_{21}C^4 + a_{22}C^3R + a_{23}C^2R^2 + a_{24}CR^3 + a_{25}R^4 + a_{26}C^3 + a_{27}C^2R \\ &\quad + a_{28}CR^2 + a_{29}R^3 + a_{210}C^2 + a_{211}CR + a_{212}R^2 + a_{213}C + a_{214}R + a_{215}\,. \end{aligned} \tag{1.21}$$

To prototype equation 1.20 and 1.21 in Matlab, "Curve Fitting Toolbox" is used to obtain the 2x6 and 2x15 parameters, using 107 points' coordinates pairs of image space R/C and world coordinates X^W/Y^W. Based on the "Goodness of fit" of transformation parameters from Matlab, the Root-Mean-Square Error (RMSE) of (X^W, Y^W) is (0.06796, 0.05638) for the 2^{nd} order polynomial, and (0.02854, 0.02343) for the 4^{th} order polynomial. As the order of polynomial goes higher, the RMSE gets smaller, and the cost of parameters' calculation gets much higher as well. After the prototyping in Matlab, the different orders of polynomial models will be applied into real-time streams transformation to get live transformed world space reconstruction. Eventually, the 4^{th} order polynomial transformation model is selected as the distortion removal mapping model, which can give an intuitive undistorted world space image while costing relative less calculations. This mapping model will be trained by coordinate-pairs of the extracted points, and then be applied to image space addresses to generate dense X^W/Y^W for all pixels.

1.4 Data Process and LUT Generation

Till now, we have collected frames of $X^WY^WZ^WRGBD$ data from RGB streams and $X^WY^WZ^WID$ from NearIR stream. The $X^WY^WZ^WRGBD$ data from RGB streams can be used for color values' alignment after the 3D reconstruction based on depth stream. Since the NearIR stream has same pixel distribution with depth stream, we will process the $X^WY^WZ^WID$ data and generate per-pixel mapping parameters, which can be saved as LUT for undistorted 3D

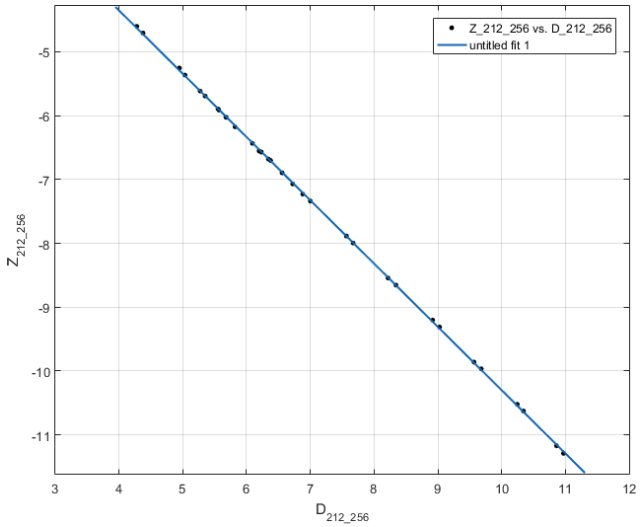

Figure 1.11: Polynomial Fitting between D and Z^W

reconstruction. From section 1.2, we know that our whole idea of a calibrated natural 3D reconstruction on GPU is to make use of per-pixel eqn. (1.9), which requires undistorted $X^W Y^W Z^W$ data and a per-pixel mapping from D to Z^W. With enough $X^W Y^W Z^W ID$ data already been collected, we will determine a per-pixel D to Z^W mapping, and then generate LUT for calibrated 3D reconstruction.

Both of D and Z^{W} are continuous data, so that their function could written as a polynomial expression, based on Taylor series. We will determine a best-fit mapping model from D to Z^{W} using Matlab. Figure 1.11 shows the polynomial fitting result in Matlab "Curve Fitting Tool" toolbox, with 32 points of DZ^{W} values (at pixel $column$=256 and row=212) from 32 frames. It is apparent that Z^{W} is linear with D. Therefore, for every single pixel, Z^{W} could be mapped from D through

$$Z^W[m,n] = e[m,n]D[m,n] + f[m,n], \tag{1.22}$$

where $[m,n]$ denotes the image address Row and Col of a pixel, e/f are the corresponding linear coefficients that help map from D to Z^{W}. With eqn. 1.22 supporting the per-pixel Z^W values and eqn. (1.9) help generating the per-pixel $X^W Y^W$ values, we found all of the six per-pixel parameters $(a/b/c/d/e/f)$ we need. We are now ready to process the collected data off-line and generate a $numDepthRows$ by $numDepthCols$ by 6 LUT.

The collected data cannot be used directly for LUT generation, because X^W/Y^W may not be well aligned and pre-processes of data are needed. Our calibration system did not require the camera's observing orientation to be along with Z^W-axis, which results to the fact that, the collected frames might be staggered when the centered dot-cluster in camera's

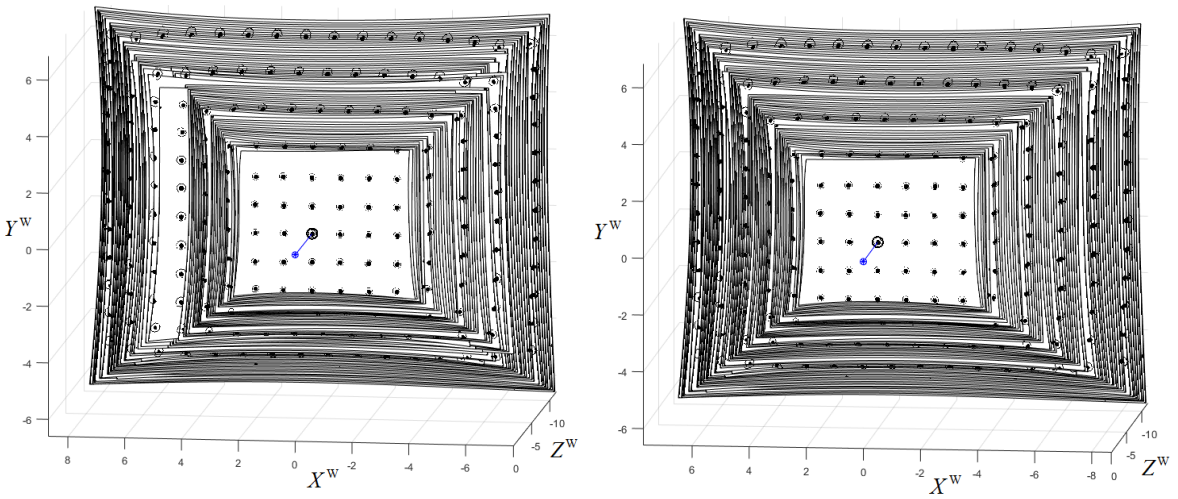

(a) Staggered (b) Unified

Figure 1.12: World Space Unification of Collected Data

FoV moves. Figure 1.12a shows the raw collected data before world space unification, which has a staggered piles of frames. In order to make the data available for generating valid per-pixel 3D reconstruction parameters, we need to unify their world space by adding or subtracting a corresponding integer to all pixels in every staggered frame, making sure the point $X^W Y^W = 0$ is at the same dot-cluster for all frames. After the data unification of world space, as shown in fig. 1.12b, we are all ready to determine the per-pixel mapping parameters $a/b/c/d/e/f$ and generate the LUT.

1.5 Alignment of RGB Pixel to Depth Pixel

Now an undistorted 3D reconstruction could be displayed with the help of the calibrated LUT. However, we have not figured out yet what the color of each pixel is. To generate a colored 3D reconstruction with a combination of a random depth sensor and a random RGB sensor, we need to align the RGB pixels to depth pixels. The intermediate between the depth sensor image space and RGB sensor image space is the world space. As long as we figure out the mapping from world space to RGB sensor image space, the color of pixel with known $X^W Y^W Z^W$ could be looked up from the RGB image space. The pinhole camera matrix M is used to map from world space to RGB image space. Using the frame data from Kinect RGB steams and Kinect NearIR streams, a Matlab prototype of RGB pixels alignment is shown in fig. 1.13a, where the RGB textured is mapped onto its corresponding NearIR image, who has same pixels with depth sensor. The total black area on the top edge and bottom edge is where the depth sensor's view goes beyond the RGB sensor's view.

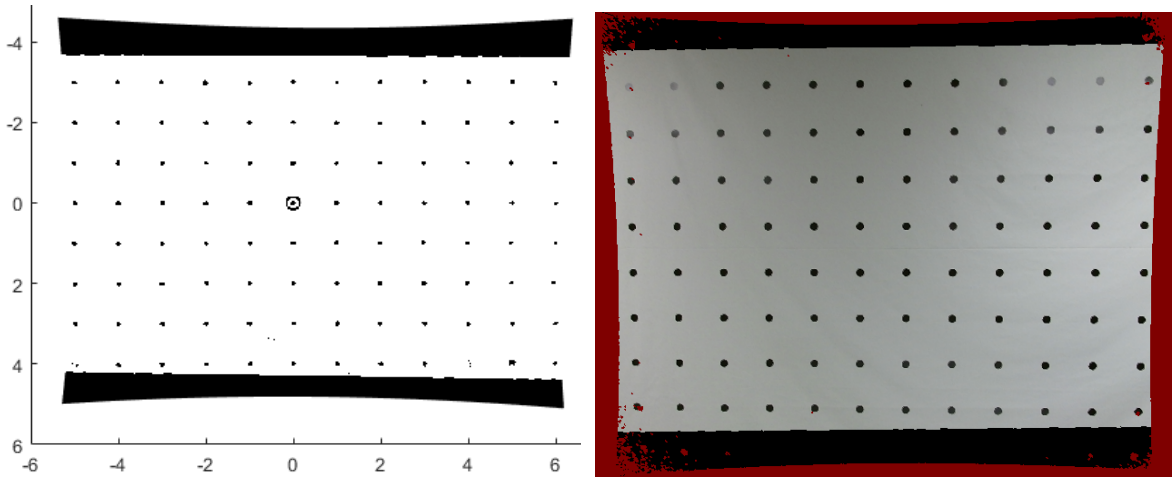

(a) (b)

Figure 1.13: Alignment of RGB Texture onto NearIR Image

Fig. 1.13b shows the screen-shot of live video after calibration with the RGB pixels aligned by a pinhole camera model M.

Chapter 2 Results of Calibration and 3D Reconstruction

2.1 Calibration Results

As discussed in section 1.3, the per-pixel calibration method requires a two-dimensional high-order polynomial model to remove lens distortions and generate estimated (X^W, Y^W)s from image space (R, C)s. In this section, we will show detailed comparisons among different order polynomial results of both Matlab prototypes and real-time live applications. Figure 2.1 shows the Matlab prototypes of the simulated original image, world space $X^W Y^W$

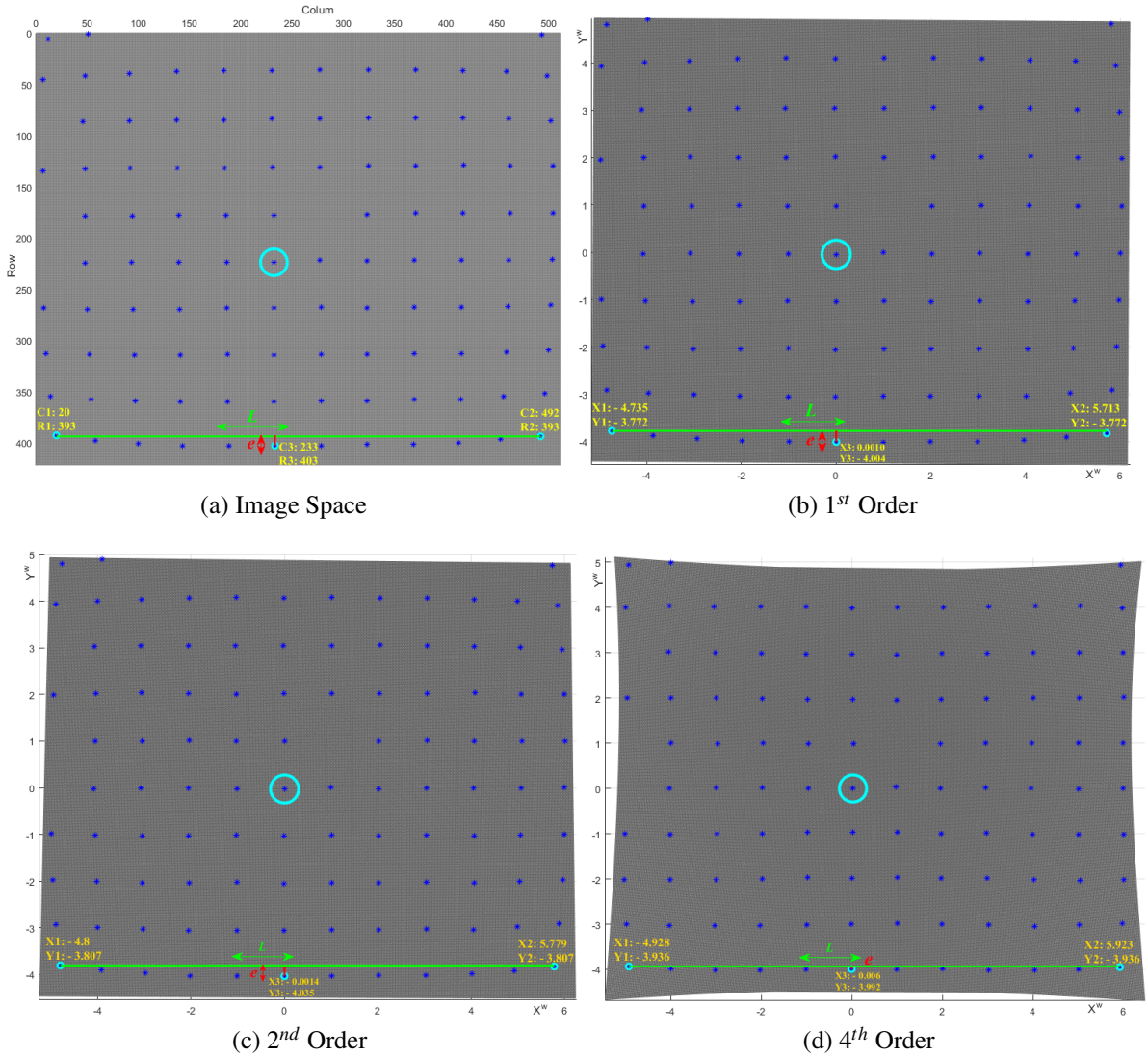

(a) Image Space

(b) 1^{st} Order

(c) 2^{nd} Order

(d) 4^{th} Order

Figure 2.1: $X^W Y^W$ Matlab Polynomial Prototype

plane result after a two-dimensional 1^{st} order polynomial transformation, 2^{nd} order polynomial and 4^{th} order polynomial transformation.

With squared-shaped distributed points (C, R)s extracted from image streams, we can recover the original distorted image in Matlab, as shown in fig.2.1a. Using a mathematical distortion (d) measurement [2]

$$d(\%) = e * 100/L, \tag{2.1}$$

we can get the original distortion $d_0 = (R3 - R1)/(C2 - C1) = (403 - 393)/(492 - 20) = 2.1\%$. Fig. 2.1b shows estimated world space $X^W Y^W$ plane after a two-dimensional 1^st order polynomial transformation, whose distortion $d_1 = (Y1 - Y3)/(X2 - X1) = [-3.772 - (-4.004)]/[5.713 - (-4.735)] = 2.2\%$. As we may have expected, the distortion d_1 is not getting smaller at all. Fig. 2.1c and fig. 2.1d show the transformed world space $X^W Y^W$ plane images after the 2^{nd} order and 4^{th} order polynomial transformation respectively, from which we can get $d_2 = [-3.807 - (-4.035)]/[5.779 - (-4.8)] = 2.1\%$ and $d_4 = [-3.936 - (-3.992)]/[5.923 - (-4.928)] = 0.516\%$. It is straightforward to tell that, d_4 is much smaller than d_0 and fig. 2.1d intuitively shows a satisfying undistorted image. From eqn. 1.20 and eqn. 1.21, we know that the second order polynomial mapping has 2x6=12 parameters, and the fourth order polynomial mapping has 2x15=30 parameters. The higher order polynomial we use, the better radial distortion we are able to correct. In the meantime, the distortion removal model will have more parameters to calculate, and need more calibrating points to train the model.

By applying those two-dimensional polynomial models into real-time streams transformation, we can get the transformed stream images. As shown in fig. 2.2, the outlines of the transformed steam images are same with Matlab prototypes in fig. 2.1. It is easy to tell that the 4^{th} order polynomial surface mapping is much better than the second order, and a higher order than 4^{th} should be more accurate. However, as the order of the polynomial mapping goes higher, the number of parameters also get larger and larger, which costs more calculations and requires more data (coordinate-pairs) for training the transformation model. Considering that a 5^{th} order polynomial mapping will have much more parameters (2x21=42) to calculate while may not enhance much accuracy, we choose the 4^{th} order polynomial as the main mapping model to get $X^W Y^W$ values from RC. Limited by the static dot pattern, fewer and fewer dot-clusters could be observed by the camera as the camera getting closer to the dot pattern. Practically, 4^{th} order calibration is replaced by 2^{nd} order to guarantee a robust software when the observed dot-clusters are too few to train the transformation model.

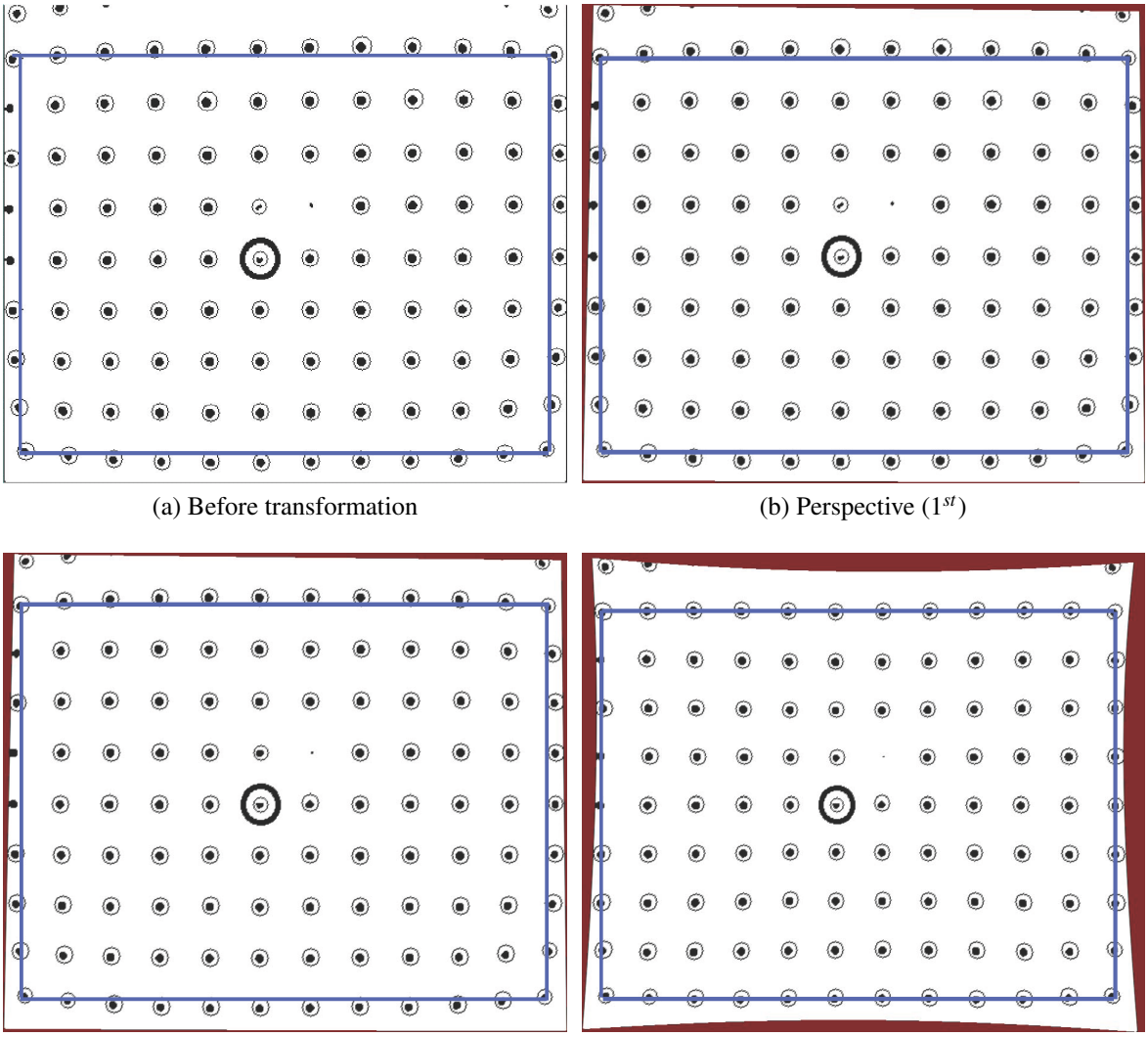

(a) Before transformation

(b) Perspective (1^{st})

(c) 2^{nd} Order

(d) 4^{th} Order

Figure 2.2: NearIR Stream High Order Polynomial Transformation

The two-dimensional high-order polynomial mapping model will be applied in the first calibration step of $X^{\mathrm{W}}Y^{\mathrm{W}}Z^{\mathrm{W}} + D$ frames data collection. Figure 2.3 shows 63 frames of collected $X^{\mathrm{W}}Y^{\mathrm{W}}Z^{\mathrm{W}}$, which gives an pyramid shape of a camera sensor's undistorted world space field of view. For each single pixel, its field of view is a beam, which could be mathematically expressed as equation. 1.9. Some sample beams are shown in fig. 2.4, whose beam equation parameters $c/d/e/f$ are determined as the best-fit totally by the collected undistorted data.

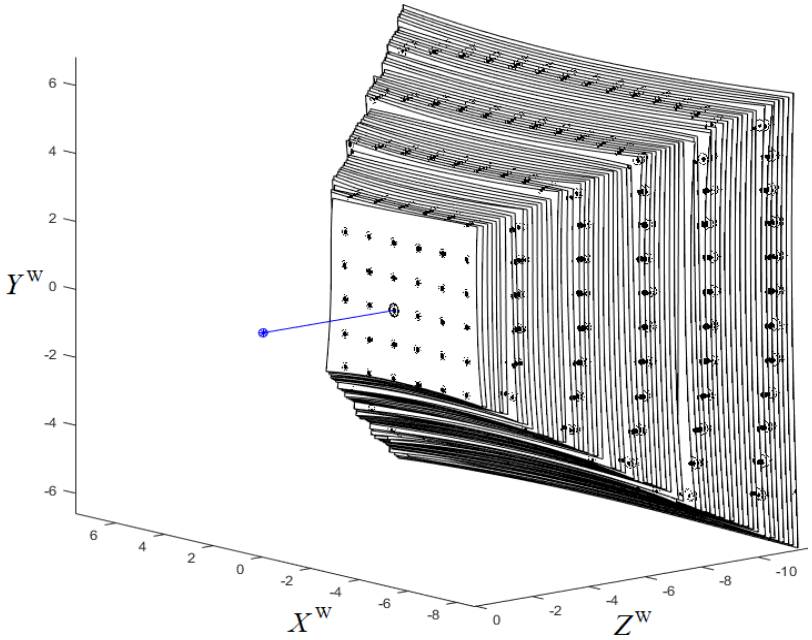

Figure 2.3: 63 Frames NearIR Calibrated 3D Reconstruction

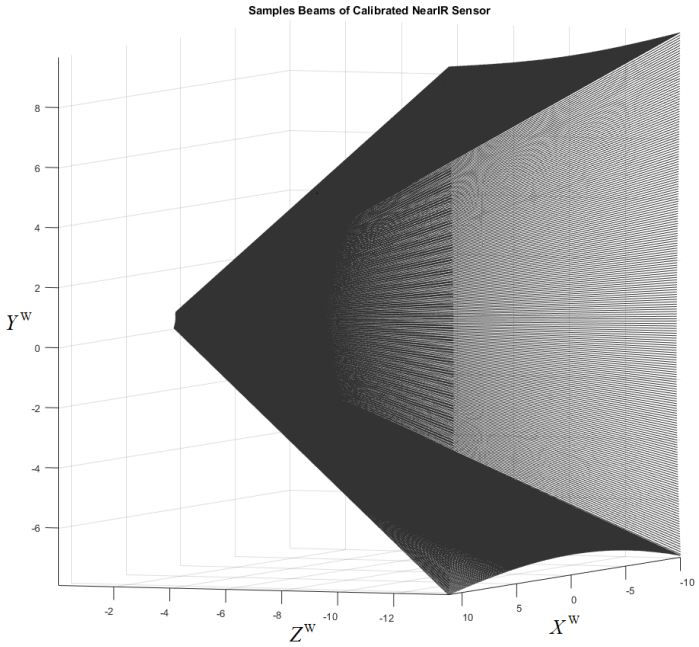

Figure 2.4: Sample Beams of Calibrated NearIR Field of View

2.2 Real-Time 3D Reconstruction on GPU

The 3D Reconstruction of undistorted $X^{\mathrm{W}}/Y^{\mathrm{W}}/Z^{\mathrm{W}}$ in real-time is the final aim of a 3D camera's calibration. In the traditional camera calibration method, which consist of one pinhole-camera matrix to generate raw world space 3D coordinates and another model for lens distortion removal, three big transformations are needed to generate the world space coordinates: from 2D distorted image space to 2D undistorted image space, then to 3D camera space, and finally to 3D world space. For every single pixel's processing, it needs 5 parameters from distortion removal model for the first step non-linear calculation, and then a 3x3 intrinsic matrix to get its camera space coordinates, and a 3x4 extrinsic matrix to finally acquire the world space coordinates. The 3D reconstruction after the traditional calibration requires a lot of calculations for every single pixel, and *depth distortion* is not corrected at all.

Using the proposed per-pixel calibration method, only three linear calculations with six parameters are needed to determine the world space coordinates for every single pixel. Two parameters e/f are utilized to generate world space Z^W, as expressed in eqn. (1.22). And the other four parameters $a/b/c/d$ are applied to get X^W/Y^W respectively based on eqn. (1.9). In this way, there is no need to calculate any non-linear equation for distortions removal, and the camera space is totally left aside. Combining two equations together, the undistorted 3D world coordinates $(X^{\mathrm{W}}, Y^{\mathrm{W}}, Z^{\mathrm{W}})$ for every single pixel could be looked up based on D from a *column*-by-*row*-by-6 look-up table. Figure 2.5 shows how lens distortions are moved, and fig. 2.6 shows how the *depth distortion* is removed by per-pixel

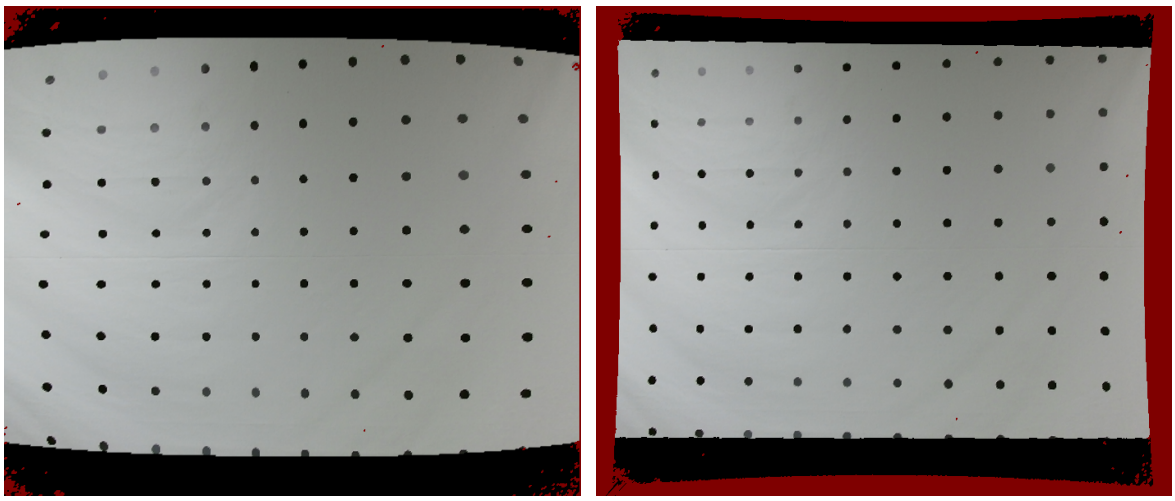

(a) Raw (Distorted) (b) Calibrated

Figure 2.5: Lens-Distortions Removal by Per-Pixel Calibration Method

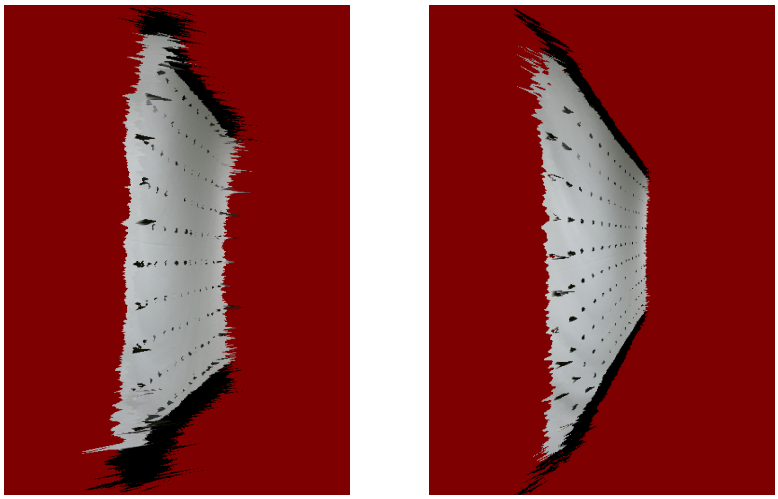

(a) Raw (b) Calibrated

Figure 2.6: Depth-Distortions Removal by Per-Pixel Calibration Method

D to Z^W mapping.

Bibliography

[1] Kai Liu. *Real-time 3-D Reconstruction by Means of Structured Light Illumination*. PhD thesis, University of Kentucky, 2010.

[2] Z. Tang, R. Grompone von Gioi, P. Monasse, and J.M. Morel. High-precision Camera Distortion Measurements with a "Calibration Harp". *Computer Vision and Pattern Recognition*, 29(10), Dec 2012.